Express letter

In situ zirconia/carbon network composite fabricated by gelcast following reduction-sintering

Yuichiro FUKUMURA,[*,**] **Deepak K. PATTANAYAK,**[**] **Chen WANGHUI,**[*,**]
Takashi SHIRAI,[**] **Masayoshi FUJI**[**] **and Feng WANG**[*,**,†]

[*]College of Materials Science and Engineering, Beijing University of Chemical Technology,
15 beisanhuan east road, Chaoyang, Beijing, 100029, P R China
[**]Advanced Ceramics Research Centre, Nagoya Institute of Technology, 3–101–1 Honmachi, Tajimi, Gifu 507–0033, Japan

Here, successful fabrication of zirconia/carbon network composite by gelcast and reduction sintering in argon gas is reported. Carbon network well distributed on the grains and the boundaries is confirmed by FE-SEM, TG–DTA, XRD, and, degree of graphitization by Raman spectroscopy. Electrical resistivity of 16.1 Ω-cm indicates that thus formed carbon network in the zirconia matrix is expected to improve the electrical conductivity of the composite system.

1. Introduction

In general, ceramic materials are added with fillers of desired characteristics to form ceramic composites where various properties such as mechanical strength, thermal or electrical conductivity etc are provided to them.[1)–3)] Recently, electro-conductive ceramics are developed that have both high mechanical strength and good electrical conductivity. These electro-conductive ceramics are often prepared by the mechanical mixing of insulating powder with conductive fillers (secondary phase) such as metals or metallic oxides to create conductive pathways or networks in the electrically insulating ceramic matrix.[4)–6)] The fabrication of these conductive pathways indicates that the percolation threshold of the conductive filler in the ceramic composite needs to be exceeded in order to obtain high electrical conductivity.[7)]

The amount of secondary phase or filler added to reach the percolation threshold depends upon its physical characteristics such as particle size and aspect ratio. Low-aspect-ratio fillers such as carbon black and graphite need to be added at least 20 vol%,[8),9)] whereas for high-aspect-ratio carbon nano tubes (CNTs) the amount of additive required is less than 12 vol%.[10),11)] However, large amount of secondary phase or conductive fillers into the ceramic matrix might degrade the intrinsic structural properties of the host ceramics. Moreover, the use of mechanical powder mixing might leads to unwanted segregation of the conductive filler within the ceramic matrix, which makes it difficult to achieve the fabrication of homogeneous conductive network structures. As a result, the composites tend to exhibit undesirable material characteristics such as anisotropy in electrical conductivity, poor reproducibility of fabrication, and unwanted grain growth. Thus, there is a need to develop alternative method where such conductive secondary phase can be formed in situ in the ceramics matrix to exhibit uniform electrical conductivity in the composite system.

Among various ceramics processing methods developed so far, gelcasting has been widely recognized as a versatile method for shaping dense or porous ceramics in its green form. The gelcasting process developed by Omatete et al. in 1991 basically requires the use of stable and high solid-loaded slurry consisting of ceramic particles, water, dispersant, monomer and cross-linker.[12),13)] The resultant slurry is subsequently cast into a mold, and, immediately after casting, in situ polymerization is initiated due to the addition of a small amount of initiator and catalyst. This polymerization process makes the slurry solidified while defining the shape of the mold of near net shape by generating macromolecular networks that hold the ceramic particles together. The successfully gelcast part consists of a well distributed three component system comprising the ceramic particles, gel matrix, and the polymer strands that cross-link throughout the entire inter-particle spaces.[14)]

The gelcast body surrounded with polymer is expected to be an attractive precursor for pyrolysis of polymer into a continuous interlink pathway of carbon when the sample is sintered in an oxygen-free atmosphere. In the present study, a novel and conductive zirconia composite was attempted to fabricate using in situ processing of gelcasting of zirconia slurry and subsequent reduction sintering in argon gas atmosphere. The properties of such sintered composite were examined.

2. Experimental procedure

In gelcasting process yttria stabilized zirconia (YSZ) powder, dispersant, monomer and initiators are used. A commercial ammonium salt of polycarboxylate (Seruna D-305) supplied by Chukyo Yushi, Japan was used as dispersant. The organic components methacrylamide (MAM) was used as a monomer, and N,N′-methylenebisacrylamide (MBAM) was used as a cross-linker. The polymerization reaction was initiated using ammonium peroxodisulfate and catalyzed by N,N,N′,N′-tetramethyl-ethylenediamine, respectively. All of these chemicals were supplied by Wako Chemical, Japan.

The gelcasting procedure used in the present study was similar to our previous studies for processing of dense and porous

---

† Corresponding author: F. Wang; E-mail: wangf@mail.buct.edu.cn

Table 1. Composition of ceramic powder and chemicals used in the gelcasting process

Components	Amount (wt%)
Zirconia (YSZ)	80.08
Distilled Water	14.88
Dispersant: Ammonium Polyacrylate	1.46
Monomer: Methacrylamide (MAM)	2.68
Cross-linker: N,N'-methylenebisacrylamide (MBAM)	0.9
Initiator: ammonium peroxodisulfate 10 mass% aq	4.68 µl/g of slurry
Catalyst: N,N,N',N'-tetramethylethylenediamine	0.3 µl/g of slurry

Fig. 1.   (a) FE-SEM photographs of fractured surface (b) cross sectional image. Carbon networks are elongated across the grain boundaries.

alumina.[15),16)] In the first step, slurry was prepared using zirconia, water, dispersant and MAM/MBAM mixture by ball milling inside a polyethylene container with zirconia balls for about 24 h. The dispersed slurry was screened to remove the zirconia balls and degassed for 10min to remove the trapped air bubbles. The degassed slurry was mixed with initiator and catalyst to initiate the free radical polymerization of monomer in a sealed chamber under a controlled N_2 gas atmosphere. The resultant mixed slurry was poured into a plastic mold and allowed for in situ solidification for overnight at 25°C in the same chamber under N_2 gas atmosphere. **Table 1** show the composition and the amount of each material used for preparing 100 gm of slurry.

These solidified green bodies were demolded and then kept in a humidity-controlled drying chamber at 25°C for 7 days in such a way that the humidity was reduced from 90 to 60% at a rate of 5% per day. The dried green bodies were sintered at 1550°C for 2 h in argon gas to ensure the oxygen-free atmosphere.

Thus prepared sintered composite sample was then characterized by various methods. Fractured surface and cross sectional image of the sintered composite sample was observed without any conductive coating by field emission scanning electron microscopy (FE-SEM; Jeol Co., Japan) in order to gain insight on the conductive path due to carbon network. For FE-SEM observation, accelerating voltage was 15 kV. The X-ray diffraction (XRD) pattern (Ultima 5, Rigaku Co., Japan) of the sintered composite sample was recorded in the 2θ range from 10 to 90° with a scan rate of 1°/min using Cu Kα radiation ($\lambda = 0.1542$ nm, 40 kV, 40 mA). Thermo gravimetry–differential thermal analysis (TG–DTA; Rigaku Co., Japan) was performed in the temperature range 20 to 1000°C at a rate of 10°C/min in the oxygen atmosphere to examine the amount of remanent carbon in the sintered composite sample. Furthermore, laser Raman spectrometry (Jasco, Japan, NRS-3100) was taken in the range of 1000 to 3000 cm^{-1} to examine the degree of graphitization of carbon. For this measurement, green laser of wave length 532 nm was used.

Electrical resistivity was measured using the two-terminal method with a square shape sintered composite sample. Two thin wires used as electrodes were connected to both sides of the plate painted with carbon paste. The contacts between wire and sample were done by heating it at 90°C for 10 min. The two other sides of the wires were connected to a current source (Advantest, R6243) with a preset d.c. current of 0.1 mA so that the voltage was obtained. The measurement was carried out at 25°C and the electrical resistivity was calculated.

3.   Results and discussions

Figures 1(a) and 1(b) show FE-SEM image of fractured surface and cross section of the YSZ green body that was sintered at 1550°C, 2 h in argon gas atmosphere. It can be seen from Fig. 1(a) that inter-connected carbon network was formed
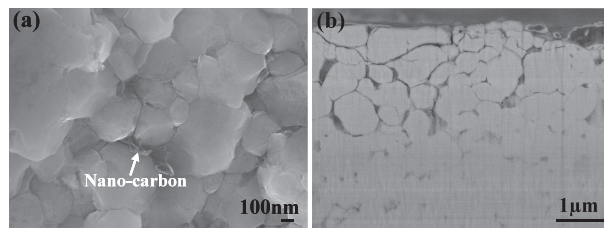
surrounding the zirconia grain. From cross sectional FE-SEM photograph [Fig. 1(b)], we can speculate that these carbon networks are extended among the grains so that they appeared to be a continuous conductive carbon path. This resulted into a 3D pathway of carbon within the YSZ composite and is expected to exhibit homogeneous electrical conductivity. In the present study, FE-SEM images were clearly observed without any conventional coating such as Os or Pt/Pd etc. This indicates that existing carbon in the YSZ matrix provides a conductive layer that prevents from charging.

Raman spectroscopy is regarded as an efficient way to characterize the structure of various carbonaceous materials with conjugated and C–C double band, and this method is widely used for the surface analysis.[17),18)] In the present study, Raman spectroscopy was performed since most parts of the sintered body were zirconia, and the carbon is thinly deposited on the surface of the zirconia particle. **Figures 2**(a) and 2(b) show the Raman spectra of YSZ sintered composite. For comparison Raman spectrum of green body is also shown. It can be seen from Fig. 2(a) that sintered sample exhibited three prominent broad peaks: D band at 1360 cm^{-1} (defect structure of graphite), G band at 1580 cm^{-1} (normal graphite structure) and D$'$ band at 1620 cm^{-1} (defect structure of graphite). The D$'$ peak is ascribed to the disorder-induced peak, and is associated with the maximum vibrational density of states. It is due to the splitting of the E2g degenerating mode in group theoretical analysis and is observed near the G peak (in-plane E2g mode) and appears like a shoulder of the G peak.[19)–21)] It is to be noted that the D$'$ peak can also be found in the Raman spectra of coke,[22)] graphene,[23)] carbon fiber,[24)] and multi-walled carbon nanotubes (MWCNTs).[25)] Additionally, the peak at 2700 cm^{-1} corresponds to the 2D band which further indicates the carbon to be existing as graphite phase as seen in Fig. 2(b). In addition, relative power unit R value (I_{1360}/I_{1580}) of these peaks was found to be 0.99. This R value indicates the degree of graphitization of the carbon. When R value is small, the degree of graphitization is very high. Thus, from the present result we can see that further graphitization might be possible at higher temperatures, and, the research is now being carried out in the laboratory.

The approximate amount of the pyrolyzed carbon is measured using simultaneous TG–DTA analysis and is shown in Fig. 2(c). It can be noted that there are two observable exothermic peaks at 525 and 760°C. The first peak is due to the oxidation of surface carbon that is directly exposed to the oxidizing gas at above 500°C, leaving a protective bed of zirconium oxide particles. Further heating at higher temperature with combination of gas diffusion process through the bed, the carbon at the bottom is completely oxidized above 750°C. The oxidation is depicted by a single weight loss in the temperature range of below 650°C, as can be seen in Fig. 2(c). From 650 to 900°C, the weight loss remained constant which indicates that the oxidation occurs at
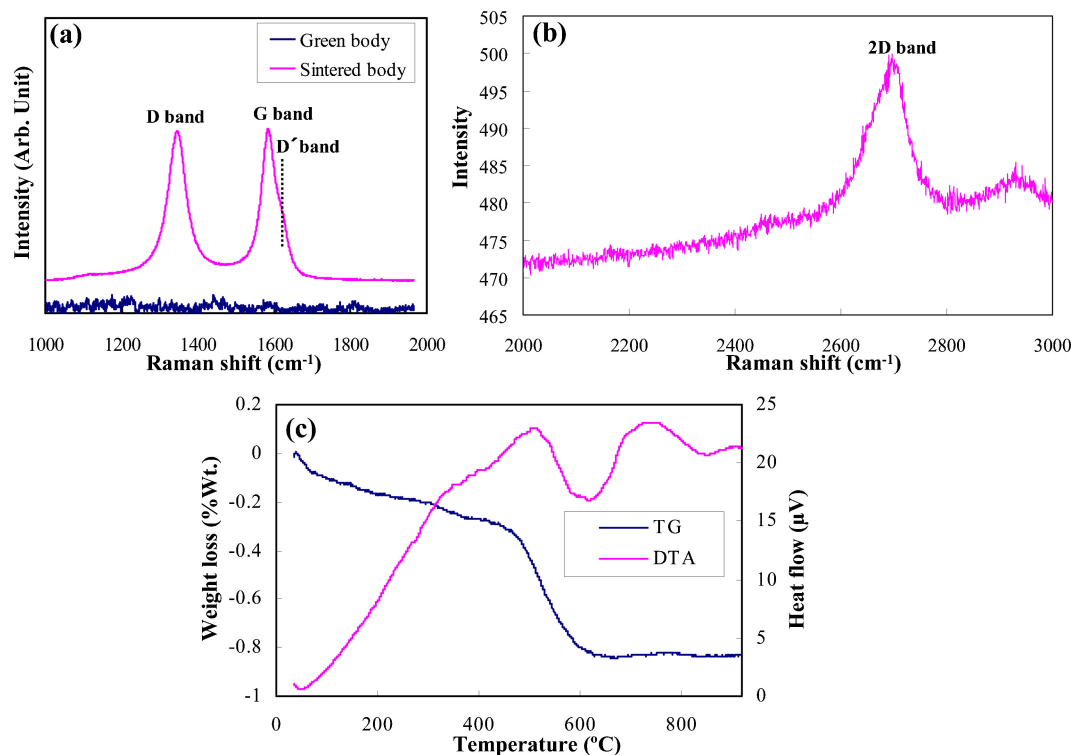
Fig. 2.　(Color online) (a) Raman spectra of green body and the sample sintered at 1550°C in argon gas atmosphere. Sintered sample shows the graphite phase corresponding to D, G and (b) 2D band at their respective wave numbers. (c) TG–DTA analysis of zirconia/carbon network composite prepared by reduction sintering of gelcast sample in argon gas atmosphere.
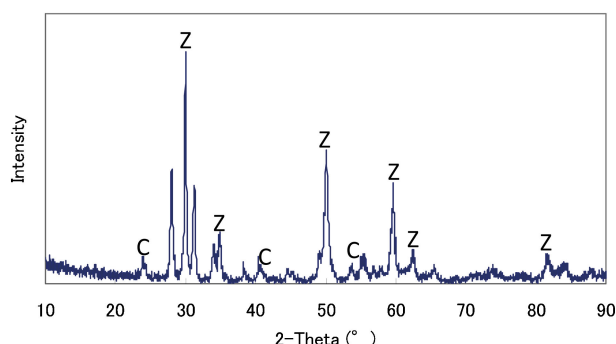

Fig. 3.　(Color online) XRD pattern of zirconia/carbon network composite prepared by reduction sintering of gelcast sample in argon gas atmosphere (C-carbon, Z-zirconia).

lower temperature. Result showed that the total pyrolyzed carbon was about 0.82 wt% upto 900°C.

Figure 3 shows the XRD pattern of YSZ composite sample that was sintered from its green body at 1550°C, 2 h in argon gas atmosphere. In general, diffraction peaks around 26, 42, 54° in 2θ are distinguishable signals correspond to hexagonal structure of graphite (002), (100), and (004), respectively.[26] In the present study, some of the YSZ peaks are overlapping in the same 2θ range. However, comparing the Raman and XRD result [Figs. 2(a) and 3], we can expect that these diffraction data correspond to the pyrolyzed carbon in the composite that exists in crystalline form rather than in amorphous. Other peaks in the XRD pattern reflect zirconia phase. The absence of other diffraction peaks in the sample indicates that other phases did not form except pure zirconia and pyrolyzed carbon that was

converted from polymer (MAM/MBAM) used in the gelcasting process.

The electrical resistivity of the sintered body was 16.1 Ω-cm. This indicates that the electrical conductivity of composite sample depends solely on concentration of remnant carbon after sintering in argon gas atmosphere. TG results showed that about 0.82 wt% weight loss when the sample was heated upto 900°C [Fig. 2(c)]. This suggests that only a small amount of carbon is required to provide an electrical conduction using the present process in comparison to metal or metal oxide based components prepared by mechanical mixing process.

The gelcasting process used in this research leads to the fabrication of dense ceramic body with uniform distribution of carbon on its surface as well as on the grain boundaries. This technique has several advantages, such as simple processing, easy to provide near-net-shape structure without any defect in the molding body. Slurry processing can easily fabricate any complicated geometry, and no special device is required. Subsequent reduction sintering of dried green body as explained in the present study converts the polymer (MAM/MBAM) into carbon instantaneously in the YSZ matrix and the resultant well distributed carbon network serves as the continuous conductive path for allowing the electric current to flow. Since the pyrolyzed carbon in the sintered gelcast sample is minimal, a proper selection of sintering gas is a necessity to avoid the reduction of carbon by chemical reaction. The use of appropriate sintering gas could possibly tailor the electrical conductivity. In this study, the argon atmosphere is promising since it renders no reaction between the pyrolyzed carbon and the host zirconia particles.

Generally, polymers are pyrolysed to form amorphous carbon in the range of 700 to 1300°C.[27],[28] However such temperature range is not enough to sinter the zirconia ceramics and also the

pyrolysed product might remain poorly conducting. It is better that these amorphous carbon should be transformed into graphite phase to obtain good electrical conductivity. Graphitization of carboneous materials occurred above 2000°C, however such graphitization temperature can be reduced in the presence of catalytic agents such as oxide ceramics.[29),30)] In the present study, similar result was noticed and the graphitization could be observed in the sample when it was sintered at 1550°C as observed in the Raman spectroscopy. However, from the peak intensity of D and G band the degree of graphitization might be further improved by increasing the sintering temperature.

We previously reported that conductive alumina could be prepared by simple gelcasting and reduction sintering in argon gas atmosphere.[16)] Conductivity decreased when the sample was sintered above 1800°C. The decrease in electrical conductivity is ascribed to the amount of carbon content in the sample. In the present study sample was sintered at 1550°C and because of the remaining carbon in the sample in the form of graphite, it showed low electrical resistivity. However, further improvement in conductivity of YSZ ceramics is now under investigation in the laboratory by increasing the sintering temperatures or surface modification methods and the detail result will be published elsewhere.

4. Conclusions

Zirconia/carbon composite are fabricated by combining gelcasting and reductive sintering of zirconia ceramics in argon gas atmosphere at 1550°C for 2 h. FE-SEM results showed carbon network distributed along the zirconia grain boundaries, Raman spectroscopy confirmed the graphitization of carbon from the D band and G band, and, further weight loss in TG results confirmed the existence of carbon in the sintered composite. This remnant carbon in the zirconia composite induces electrical conductivity to zirconia ceramics.

References

1) "Handbook of Ceramics Composites", Ed. by N. P. Bansal, Kluwer Academic Publishers (2005).
2) S. Salehi, O. Van der Biest and J. Vleugels, *J. Eur. Ceram. Soc.*, 26, 3173–3179 (2006).
3) A. Bellosi, G. D. Portu and S. Guicciardi, *J. Eur. Ceram. Soc.*, 10, 307–315 (1992).
4) R. G. Duan, J. D. Kuntz, J. E. Garay and A. K. Mukherjee, *Scr. Mater.*, 50, 1309–1313 (2004).
5) Y. Zhang, L. Wang, W. Jiang, L. Chen and G. Bai, *J. Eur. Ceram. Soc.*, 26, 3393–3397 (2006).
6) I. Kimura, N. Hotta, Y. Hiraoka, N. Saito and Y. Yokota, *J. Eur. Ceram. Soc.*, 5, 23–27 (1989).
7) F. Lux, *J. Mater. Sci.*, 28, 285–301 (1993).
8) C. S. Balazsi, Z. Konya, F. Weber, L. P. Biro and P. Arato, *J. Mater. Sci. Eng. C*, 23, 1133–1137 (2003).
9) S. Rul, F. Lefevre-Schlick, E. Capria, C. Laurent and A. Peigney, *Acta Mater.*, 52, 1061–1067 (2004).
10) K. Ahmad, W. Pan and S. L. Shi, *Appl. Phys. Lett.*, 89, 133122 (2006).
11) G. D. Zhan, J. D. Kuntz, J. E. Garay and A. K. Mukherjee, *Appl. Phys. Lett.*, 83, 1228–1230 (2003).
12) A. C. Young, O. O. Omatete, M. A. Janney and P. A. Menchhofer, *J. Am. Ceram. Soc.*, 74, 612–618 (1991).
13) O. O. Omatete, M. A. Janney and R. A. Strehlow, *J. Am. Ceram. Soc. Bull.*, 70, 1641–1649 (1991).
14) S. Ghosal, A. Emami-Naeini, Y. Harn, B. S. Draskovich and J. P. Pollinger, *J. Am. Ceram. Soc.*, 82, 513–520 (1999).
15) M. Takahashi, K. Adachi, R. L. Menchavez and M. Fuji, *J. Mater. Sci.*, 41, 1965–1972 (2006).
16) R. L. Menchavez, M. Fuji and M. Takahashi, *Adv. Mater. (Deerfield Beach Fla.)*, 20, 2345–2351 (2008).
17) S. Banerjee, T. Hemraj-Benny and S. S. Wong, *Adv. Mater. (Deerfield Beach Fla.)*, 17, 17–29 (2005).
18) K. N. Kudin, B. Ozbas, H. C. Schniepp, R. K. Prud'homme, A. I. Aksay and R. Car, *Nano Lett.*, 8, 36–41 (2008).
19) T. Jawhari, A. Roid and J. Casado, *Carbon*, 33, 1561–1565 (1995).
20) G. A. Zickler, B. Smarsly, N. Gierlinger, H. Peterlik and O. Paris, *Carbon*, 46, 3239–3246 (2006).
21) F. C. Tai, C. Wei, S. H. Chang and W. S. Chen, *J. Raman Spectrosc.*, 41, 933–937 (2010).
22) M. Kawakami, T. Karato, T. Takenaka and S. Yokoyama, *ISIJ Int.*, 45, 1027–1034 (2005).
23) R. Arsat, M. Breedon, M. Shafiei, P. G. Spizziri, S. Gilje, R. B. Kaner, K. Kalantar-Zadeh and W. Wlodarski, *Chem. Phys. Lett.*, 467, 344–347 (2009).
24) S. S. Tzeng, *Carbon*, 44, 1986–1993 (2006).
25) E. F. Antunes, A. O. Lobo, E. J. Corat, V. J. Trava-Airoldi, A. A. Martin and C. Verissimo, *Carbon*, 44, 2202–2211 (2006).
26) A. L. Ocampo, M. Miranda-Hernandez, J. Morgado, J. A. Montoya and P. J. Sebastian, *J. Power Sources*, 160, 915–924 (2006).
27) K. Laszlo, A. Bota and I. Dekany, *Carbon*, 41, 1205–1214 (2003).
28) M. Monthioux and O. Delverdier, *J. Eur. Ceram. Soc.*, 16, 721–737 (1996).
29) J. K. Yu, S. Ueno, H. X. Li and K. Hiragushi, *J. Eur. Ceram. Soc.*, 19, 2843–2848 (1999).
30) A. Oya and H. Marsh, *J. Mater. Sci.*, 17, 309–322 (1982).